Arabian Journal for Science and Engineering (2019) 44:4693–4702
https://doi.org/10.1007/s13369-018-3519-1

RESEARCH ARTICLE - CIVIL ENGINEERING

Performance of Cement–Soil Pile Composite Foundation with Lateral Constraint

Youping Wu[1,2,3] · Keneng Zhang[1,2] · Liangming Fu[3] · Jie Liu[4] · Jie He[4]

Received: 2 March 2017 / Accepted: 6 August 2018 / Published online: 28 August 2018

Abstract
A lateral constraint can effectively reduce the foundation settlement and reduce the stress of a pile shaft in a foundation treatment. Based on the characteristics of railway engineering and soft soil engineering, this paper studied the influence that lateral constraint exerted on the stress and settlement of cement–soil pile composite foundation by using indoor large-scale model testing. A comparative analysis of the stress and settlement of cement–soil pile and soil following load change is performed, and the mechanism of lateral constraint is discussed. The results show that the settlement of the pile top with lateral constraint is 8–30% lower and that of the soil around the pile is 7–9% lower when comparing the settlement values of the composite foundation with and without lateral constraint in the cement–soil pile composite foundation. The stress value of the pile top in the composite foundation with the lateral constraint is 18–32% lower than that without any lateral constraint. The stress of the cement–soil pile shaft first increases and then decreases with the depth, and the maximum stress appears at 0.15–0.35 times the pile length from the top. The position of the maximum axial force of the pile without a lateral constraint is lower than that with a lateral constraint, and the maximum stress value of the pile is 112–153% of the stress value of the pile top. Therefore, setting the lateral constraint can effectively stop the lateral deformations of soft soil, reducing the settlement of the composite foundation and pile shaft stress.

Keywords Lateral constraint · Cement–soil pile · Composite foundation · Settlement · Stress

1 Introduction

Cement–soil piles [1] or cement–soil pile composite foundations [2] have been used in high-speed railway (250 km/h) subgrade treatments and enjoy high reinforcing efficiency and great economic benefit. With the rapid development of high-speed railway construction, the number of railways with 350 km/h speeds has gradually increased. Out of the 12 high-speed railways that began in 2016, ten were designed for speeds of 350 km/h [3]. Methods for adopting low-cost cement–soil pile composite foundation in high-speed railway foundation treatment remain to be solved. The faster the train runs, the higher the requirements of railway subgrade settlement control will be. The settlement of the foundation is closely associated with lateral displacement of soil [4–11]: Tavenas [4,5] studied the relationship between lateral deformations and loading rate during construction by soft foundation filling tests. Handy [5] found that high lateral pressure can increase the load value of the foundation. Wang et al. [6,7] provided a calculation formula for a settlement correction coefficient that considers dilatancy. The correction coefficient is mainly related to the relative embankment height, soft soil porosity ratio and burial depth. Smadi [8] found that the maximum lateral displacement at the toe of the stable embankments is approximately equal to the total settlement during construction and approximately 20% of the total settlement after construction. Loganathan et al. [9] found that the maximum lateral displacement of an embankment at the loading stage was 0.28 times the maximum settlement at the centre of the embankment. Han et al. [10] established

✉ Youping Wu
wwuyn@163.com

1 Department of Geological Engineering, School of Geosciences and Info-Physics, Central South University, Changsha 410083, China

2 Key Laboratory of Non-Ferrous Resources and Geological Hazard Detection, Changsha 410083, China

3 PowerChina Zhongnan Engineering Co. Ltd., Changsha 410014, China

4 School of Civil Engineering, Hunan University of Technology, Zhuzhou 412008, China

Table 1 Physical mechanical index of soils

Serial	Compression modulus/MPa	Water content/%	Density/ (g/cm^3)	Plastic limit	Liquid limit	Cohesiveness/ kPa	Internal friction angle/°
Test 1	1.856	28.4	17.6	29.9	47.0	10.8	5.6
Test 2	2.89	23.5	18.1	21.2	42.7	13.6	12.5

a lateral displacement–settlement model based on the equal volume method, deriving the settlement formula to calculate lateral displacement, and concluded that the settlement caused by lateral displacement equals 20% of the total settlement through a test in the Lan Xu highway. Liu et al. [11] studied the factors contributing to lateral deformations of soft soil in cement–soil pile composite foundations.

To restrain the lateral displacement, Wu [12] made a systematic study of the composite foundation of a grid structure. To reduce the rip-rap out of the subgrade, Bai et al. [13] proposed piling 2 to 3 rows of stakes into the toe of the slope on both sides of subgrade. Both the grid structure and rows of stakes involve large engineering planning. To effectively limit the lateral deformations of soft soil, the method of setting piles with constraint on the sides of the embankment along the railway is proposed, considering the engineering characteristics of soft soil and the working characteristics of railway engineering, which aims to reduce subgrade settlement and improve the stability of soft soil subgrade. In this paper, a composite foundation comparative model experiment is performed to study the settlement characteristics of cement–soil pile composite foundations with lateral constraint.

2 Model Experiment

2.1 Laboratory Experiment

The model test of the soil–cement pile composite foundation with a lateral constraint was performed in two groups (Test 1 and Test 2). Test 1 was conducted in an iron box with dimensions of 2000 mm × 2000 mm × 1500 mm (length × width × height), and the geometric similarity ratio (model size to prototype size ratio) of the piles was 1:8, while Test 2 was conducted in a trough with dimensions of 6000 mm × 3000 mm × 4000 mm (length × width × height) in the laboratory, and the geometric similarity ratio of the piles was 1:6. As the experimental model cannot fully satisfy the similarity theorem, the effect of the lateral constraint on the properties of composite foundation was studied by comparison test. The two tests were essentially identical in content and process, both of which filled in the iron box and trough with soft clay in layers. The soil required for the model test was taken from the site and subjected to air drying, crushing, and sieving with a sieve of 5-mm grids; then, the moisture content was tested, with an allocation of water at 30% water content (considering water loss of 5%). To fully soak the soil, the mixture was covered with thin film for 7 days. The soil was filled in at a thickness of 200 mm per layer, and the compaction work was determined by the compaction test. Then, it was rammed by an improved dynamic penetrator (welding a 200 mm × 200 mm × 20 mm steel plate at the bottom of the metal cone), which was compacted by blows from a slide hammer with a mass of 63.5 kg falling through a distance of 760 mm. The ramming was performed twice, five hits each time with the overlapping length of 160 mm each hit. After filling, the top of the filling soil was covered with thin film to retain moisture, which formed the pile after deposition for 28 days.

Table 1 shows the mechanical and index properties of the material. The plasticity index and the liquid limit in Table 1, along with the results from sieving (more than 50% passes the No. 200 U.S. standard sieve), show that the soil types belong to silty clay (Test 1) and lean clay (Test 2), respectively, according to the Standard Practice for Classification of Soils for Engineering Purposes (ASTM D2487-17). To understand the mineral composition of clay, the soil samples of Test 2 were tested through X-ray diffraction (XRD), and for the main composition of clay minerals obtained, see Fig. 1. From Fig. 1, it can be analysed that the clay minerals are the main components of quartz, muscovite, koktaite, etc., and the main chemical components are SiO_2, Fe_2O_3, Al_2O_3, etc.

The cement–soil mixture that was made for the cement–soil pile was mixed clay with cement. The same clay was used in the soil–cement mixture and filling soil, for which the air drying, crushing, screening and measuring of the moisture content of the soil are similar to those of the former, which was only sieved with a sieve of 1-mm mesh to accelerate the interaction with cement and avoid a great difference of cement–soil mixture. Ordinary Portland cement was used, of which the strength grade was 32.5 according to China General Cement Code (GB175-2007), and the dosage was $\alpha_w = 10\%$. The moisture of the mixture achieved the optimal 18%. The compressive strength of cement–soil was 718.2 kPa (Test 1) and 745.6 kPa (Test 2) after a curing period of 28 days. The cement–soil pile needs to be pre-pore-formed, and pore forming was made through a long wooden pile with the same diameter as the cement–soil pile driven into the design depth of the cement–soil pile and then pulled out.

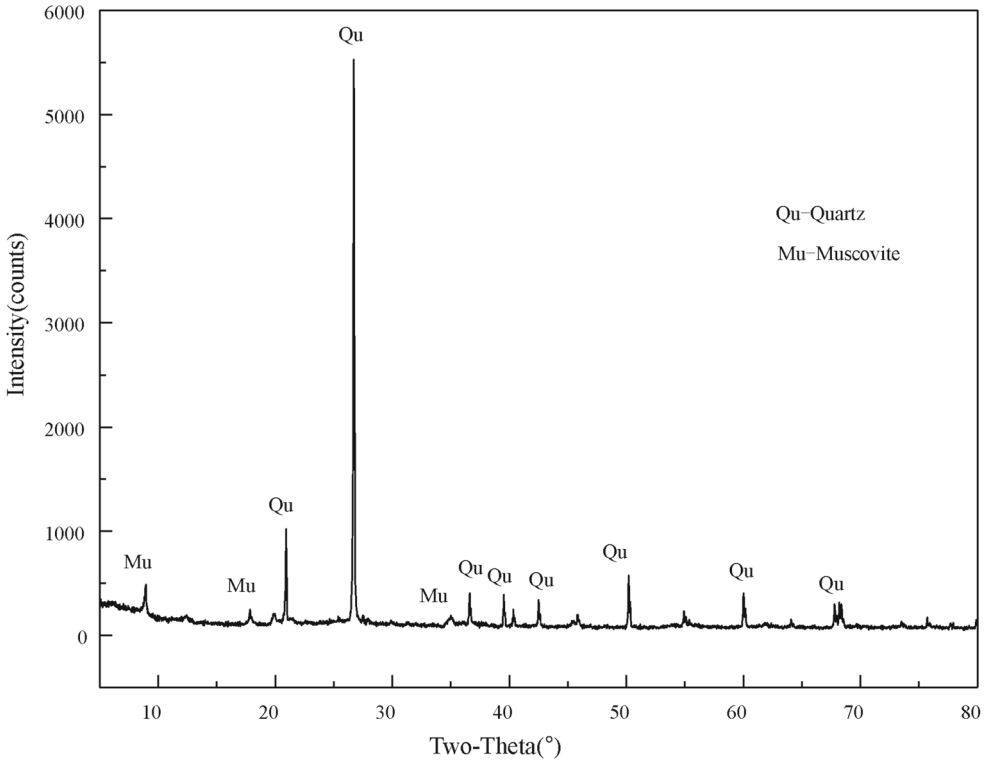

Fig. 1 The X-ray diffraction curves

Table 2 Parameters of the model pile

Serial	Number	Quantity	Diameter/mm	Length/mm	Material
Test 1	1	18	75	900	Cement–soil
	2	6	75	1500	Chinese Fir
Test 2	3	18	100	1200	Cement–soil
	4	10	75	1800	Chinese Fir

Table 3 Basic index properties of Chinese Fir

Basic index	Unit	Quantity
Moisture content at fibre saturation point	%	27.5
Density at fibre saturation point	g/cm^3	0.728
Compressive strength parallel to grain	MPa	31.7
Bending strength	MPa	63.5
Modulus of elasticity in static bending	MPa	9.8×10^3
Mean compressive strength perpendicular to grain	MPa	25.8
Mean modulus of elasticity perpendicular to grain	MPa	5.0×10^2

The cement soil pile was made by ramming the cement–soil mixture into a borehole in layers, with a compaction factor of 0.9. Chinese Fir was used for the pile, with the constraint parameters given in Table 2. The basic index properties of Chinese Fir used in Test 2 are given in Table 3. The central three piles of each group of piles served as test piles, and the pile spacing was twice the pile diameter in Test 1 and three times the pile diameter in Test 2. Pile bottom stress was tested by an earth pressure box, and the pile shaft stress tests adopted a PVC pipe paste strain gauge. The specific process is shown in reference [14].

The load tests were carried out 29 days after forming the pile, and the composite foundation load tests with and without constraint were performed simultaneously. The load plate size (steel plate) for loading was 500 mm × 500 mm × 14 mm in Test 1 and 707 mm × 707 mm × 20 mm in Test 2. The tests adopted the fast maintenance load method. Before the test, the surface of the cement soil pile at the top of the loading area should be cleaned and smoothed, as shown in Fig. 2 and Fig. 3. Then, the settlement marks and the dial gauges were arranged, and the initial reading of the dial gauges was performed, as shown in Figs. 4 and 5. A gravel cushion was packed on the load area. Figure 3a, b shows the settlement mark and loading area, and Fig. 3c shows the loading, adopting the concrete test block as the load, where each load was approximately 60 kg (2.4 kPa) in Test 1. According to the s–lg$t$ curve, it was determined that the load was stopped when the load was 14.7 kPa (pile group without constraint); at this

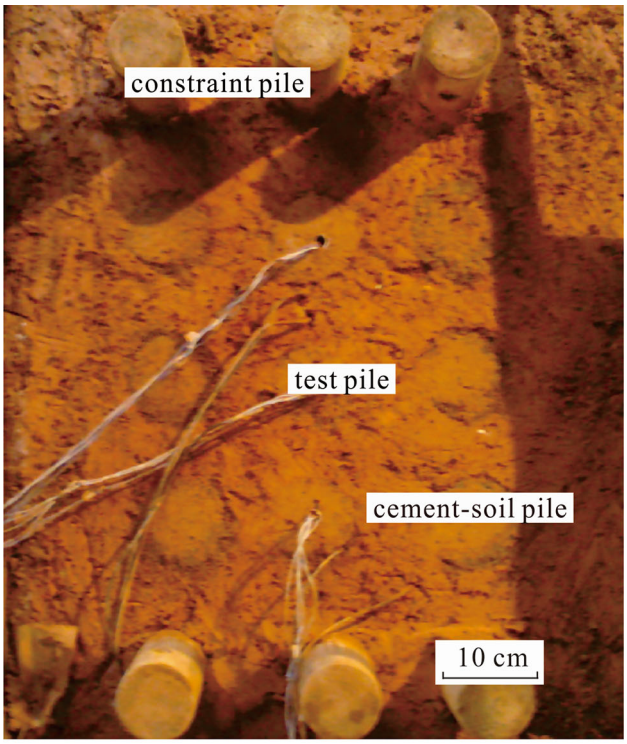

(a)

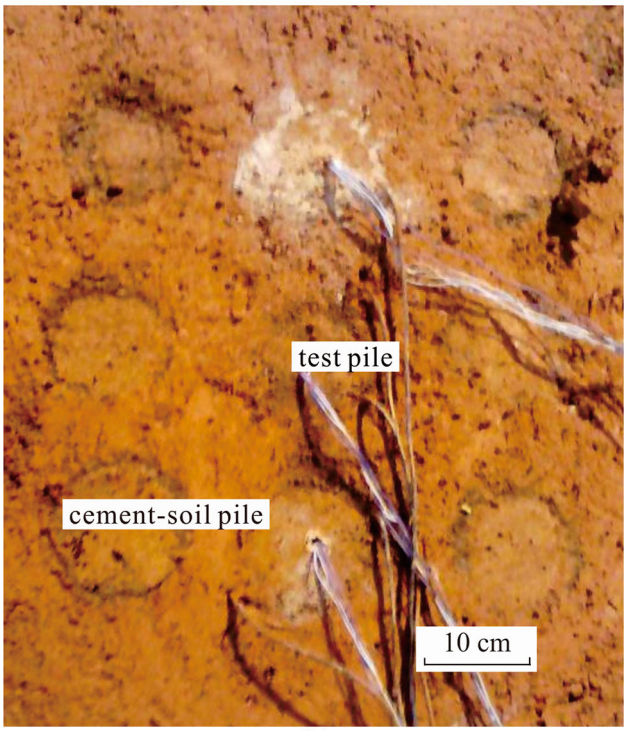

(b)

Fig. 2 Picture of group piles with or without lateral constraint in Test 1. **a** Picture of the pile group with lateral constraint. **b** Picture of the pile group without lateral constraint

time, the loading of the pile group with a lateral constraint was 14.5 kPa in Test 1. Each load was 8 kPa, and the total load was 56 kPa in Test 2.

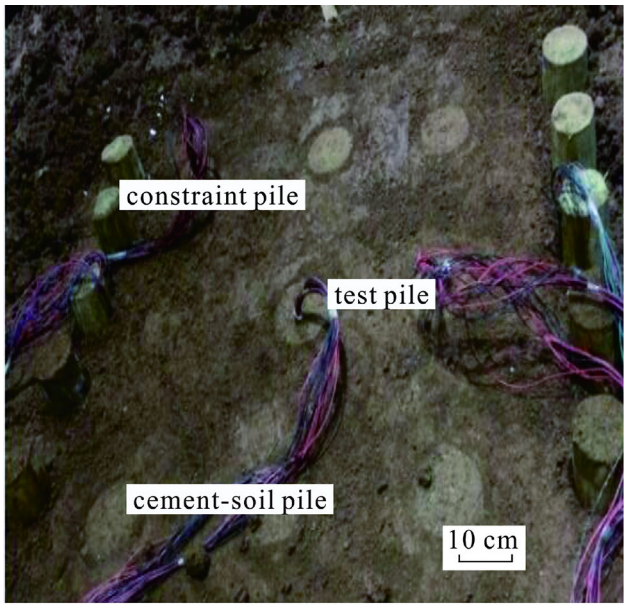

(a)

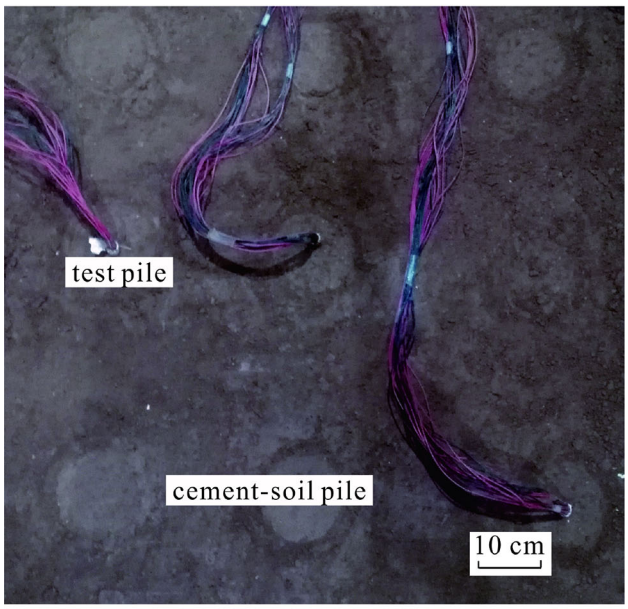

(b)

Fig. 3 Picture of group piles with or without lateral constraint in Test 2. **a** Picture of the pile group with lateral constraint. **b** Picture of the pile group without lateral constraint

3 Results

3.1 Settlement Characteristics

Figure 6 shows the pile and soil load sedimentation; the top value of the centre pile is measured at position #2 (shown in Figs. 4a, 5, similarly hereinafter), and the top value of the mid-side pile is the average of the measured values at positions #1 and #4 (without considering the second group

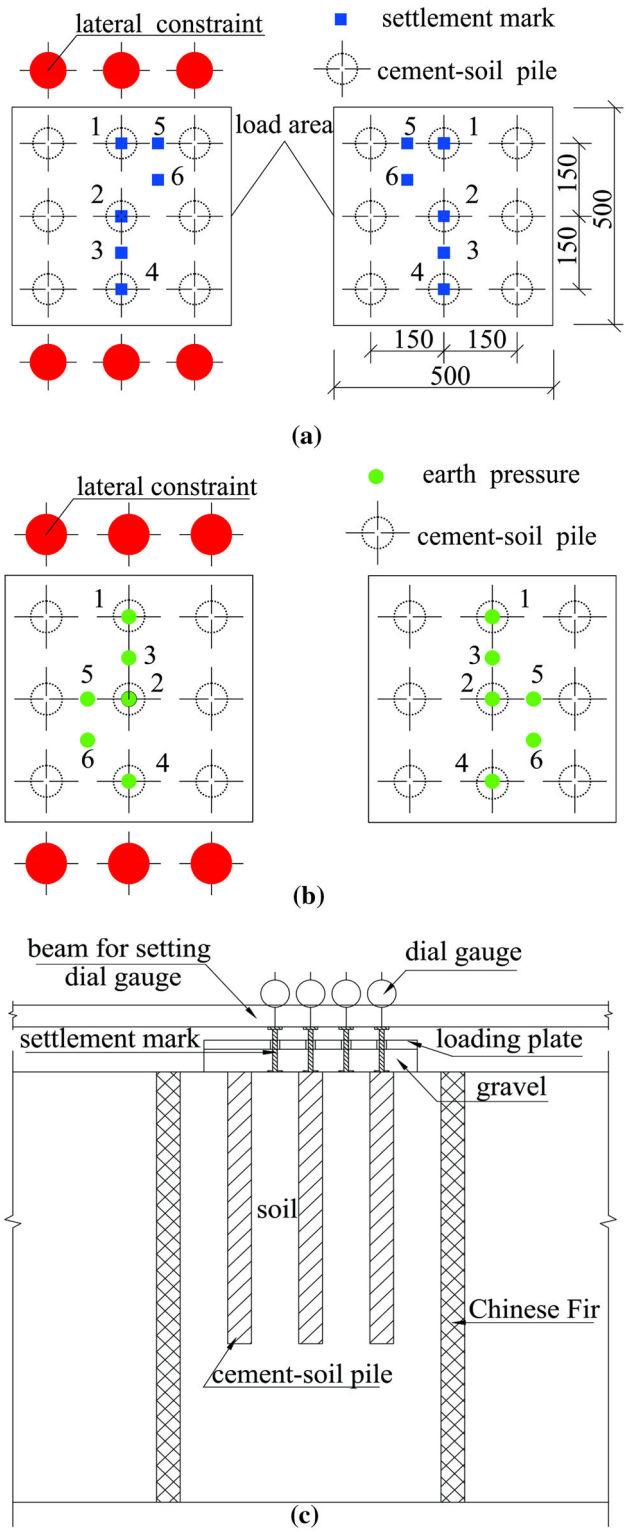

Fig. 4 Test 1 of the composite foundation. **a** Sketches showing the settlement marks and the loading area. **b** Sketches showing the earth pressure cells and the loading area. **c** Test arrangement

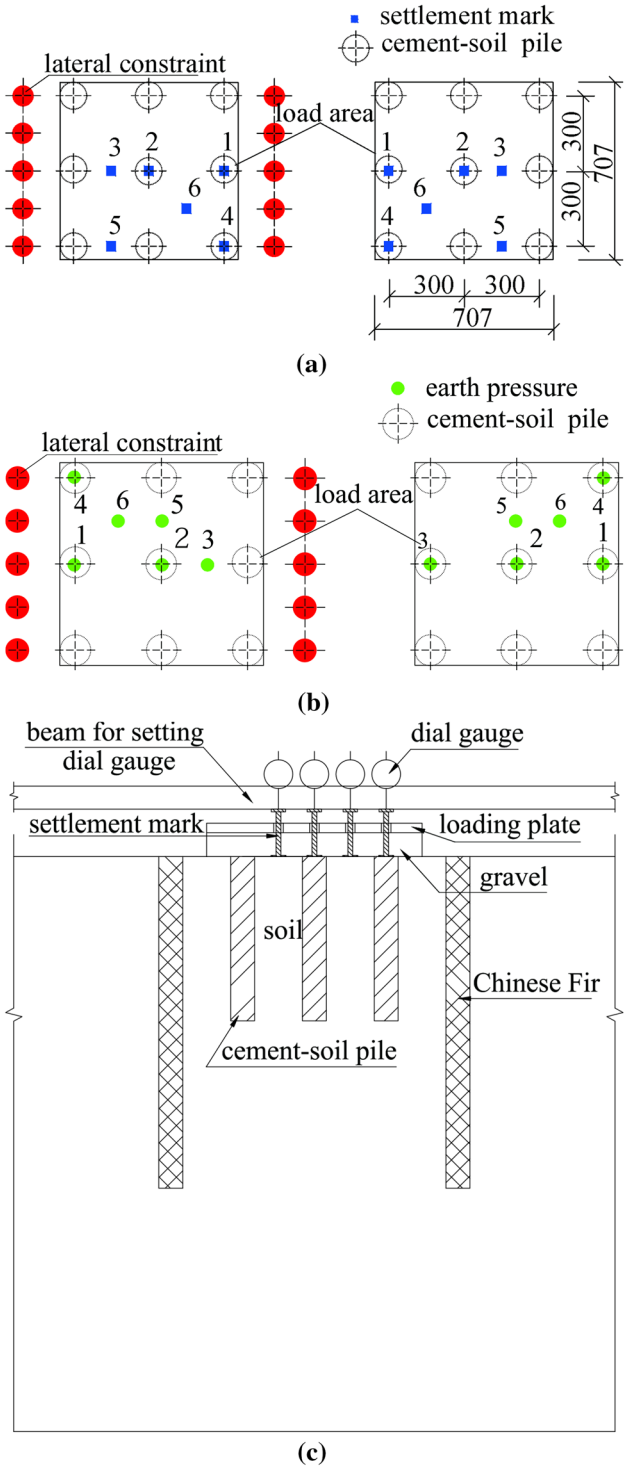

Fig. 5 Test 2 of the composite foundation. **a** Sketches showing the settlement marks and the loading area. **b** Sketches showing the earth pressure cells and the loading area. **c** Test arrangement

#4). The soil surface value is the average of the measured values at positions #3, #5 and #6.

As shown in Fig. 6a, (1) the settlement value of the soil is larger than that of the pile, with or without lateral constraint. The settlement value of the centre pile is larger than that of the mid-side pile, and the difference increases with

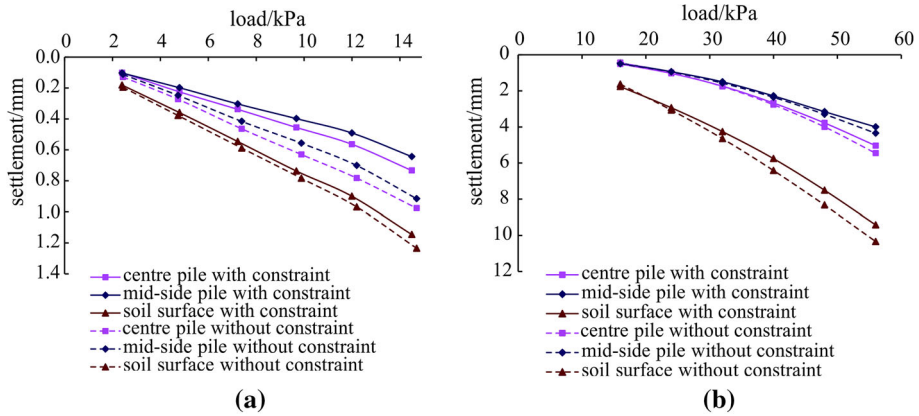

Fig. 6 Load–settlement curve of piles and the soil surface. **a** Test 1. **b** Test 2

Table 4 The settlement ratio of the cement–soil composite foundation

	With later constraint	Without later constraint
Centre pile top/soil	0.64	0.79
Mid-side pile top/soil	0.56	0.74
Centre pile top	0.75	1.0
Mid-side pile top	0.7	1.0
Soil surface	0.93	1.0

increasing load. (2) A comparison between settlement of the cement–soil pile and soil with and without lateral constraint shows that the settlement of the pile top and soil with lateral constraint is less than that without lateral constraint, and the difference is greater with increasing load. Table 4 shows the settlement ratio of the cement–soil composite foundation, and it can be seen that (1) even under the last load, the settlement value of the centre pile top is 64–79% of the soil, and the settlement value of the mid-side pile top is 56–74% of the soil; (2) under the last load, the comparison between the settlement with and without constraint shows that the top value of the centre pile is 25% less than that of the latter, the top value of the mid-side pile is 30% lower than that of the latter, and the soil around the pile is 7% less than that of the latter.

As shown in Fig. 6b, the settlement law is similar to that of Fig. 6a. Under the last load, the settlement value of the centre pile top is approximately 53% that of the soil, and the settlement value of the mid-side pile top is 42–45% that of the soil. The comparison of settlement between with constraint and without constraint shows that the top value of the centre pile is 8% less than that of the latter, the top value of the mid-side pile is 8% less than that of the latter, and the soil around the pile is 9% less than that of the latter. Whatever the pile is with or without lateral constraint, the ratio between settlement of the pile top and of the soil is quite close in Test 2, but there is a greater difference in the ratio in Test 1 after comparing the two graphs.

3.2 Pile Top Stress

Figure 7 shows that the pile top stress of the cement–soil pile changes with the change in the load. Figure 7a shows that the increase in the pile top stress of the composite foundation with lateral constraint is smaller than that without lateral constraint. Under an equal load, the stress value of the pile top is 68–88% of that without lateral constraint, and the ratio of the pile top stress decreases with an increase in the load. At the same composite foundation, the stress of the mid-side pile top is lower under an equal load, and the difference increases with the increase in the external load.

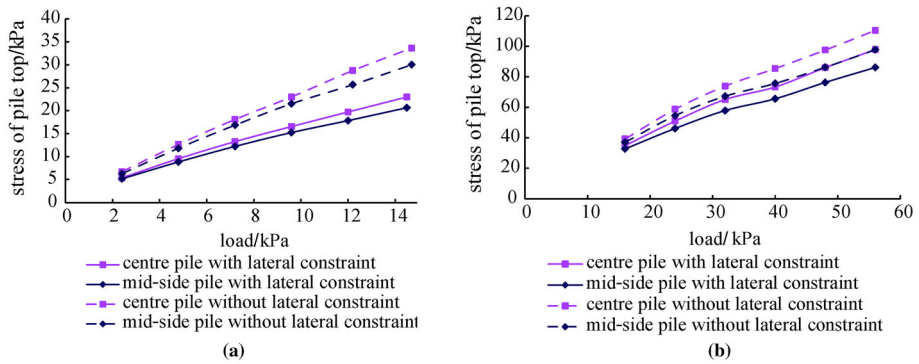

Fig. 7 Cure of pile top stress. **a** Test 1. **b** Test 2

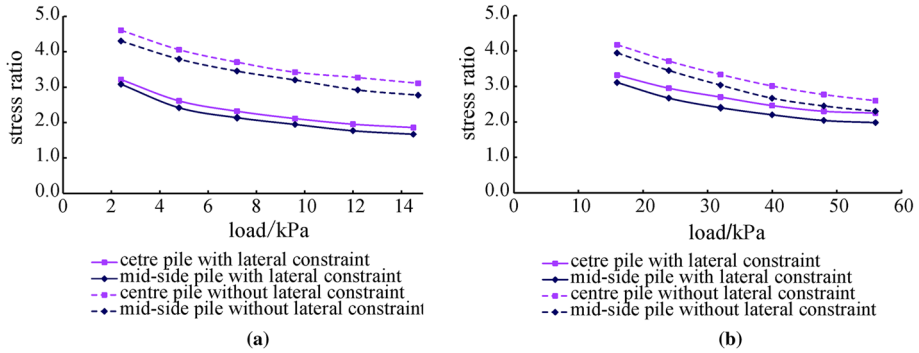

Fig. 8 Curve of pile–soil stress ratio loading. **a** Test 1. **b** Test 2

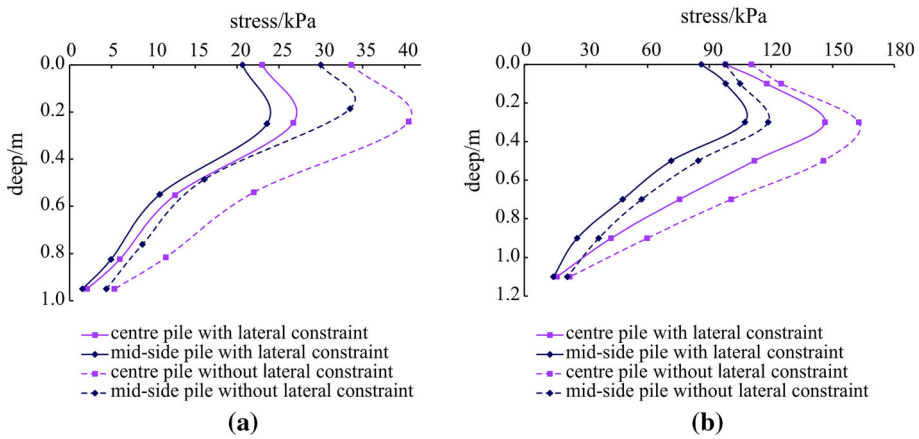

Fig. 9 Stress–deep curve of the cement–soil pile. **a** Test 1. **b** Test 2

As shown in Fig. 7b, the increase in the pile top stress is smaller than that without any constraint with an increase in the load. Under equal loads, pile top stress is 82–89% of that without lateral constraint. A comparison of the above two graphs shows that the increased rate of pile top stress without lateral constraint is higher than that with lateral constraint when the soil strength is small and that when the soil strength increases, the increased rate of the pile top with the constraint is approximately the same as that without the lateral constraint.

3.3 Pile–Soil Stress Ratio

Figure 8 shows that the pile–soil stress ratio of the centre pile and mid-side pile varies with load. As shown in Fig. 8a, the pile–soil stress ratio decreases with an increase in the load, first drastically and then slightly. It also shows that the load sharing by the pile and soil in the cement–soil pile composite foundation is variable, decreasing with increasing load. The pile–soil stress ratio of the centre pile is larger than that of the mid-side pile. The pile–soil stress with constraint is 60–70% of that without the constraint.

In Fig. 8b, we can see that the pile–soil stress ratio decreases with the increase in the load. The stress ratio of the centre pile is larger than that of the mid-side pile. The pile–soil stress ratio with constraint is 79–86% of that without any constraint. With the increase in load, the two stress ratios begin to approach each other.

3.4 Pile Shaft Stress

Figure 9 shows the variation of pile shaft stress of the centre pile and mid-side pile with the depth. As shown in Fig. 9a, the pile shaft stress of both the centre pile and mid-side pile with constraint is 30–50% lower than that without constraint at any depth. In the same pile group, the stress value of the mid-side pile is smaller than that of the centre pile. As shown in Fig. 8a, the maximum value of the pile shaft stress is not at the pile top but at a depth from the top of the pile, which is approximately 0.15–0.35 times the length of the pile from the top. When the depth is exceeded, the pile shaft stress begins to decrease, first greatly and then slightly.

As shown in Fig. 9b, under the last load, the maximum pile shaft stress is 1.38–1.53 times that of the pile top, which lies at 0.25–0.35 times the pile length from the top. The stress on the pile top with constraint is 88–89% of that without any constraint. When the pile shaft stress reaches the maximum, the stress with constraint is 74–80% of that without any constraint. Therefore, the pile shares less load in a composite foundation with lateral constraint, and the maximum stress of the pile shaft can also be reduced, which is beneficial for lessening the pile shaft stress.

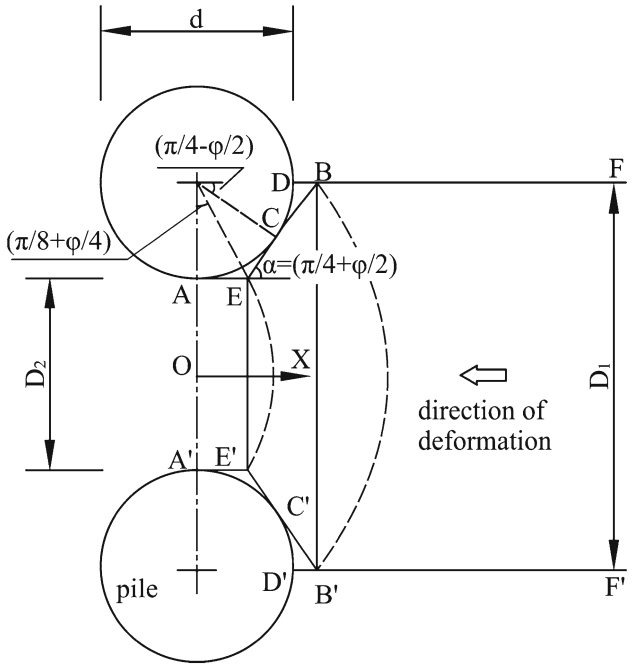

Fig. 10 State of plastic deformation in the ground just around piles (Ito and Matsui [15])

4 Discussion

4.1 The Mechanism of Constraint Pile

The pile with constraint is mainly subjected to horizontal force in the composite foundation, which can be divided into two parts: the horizontal load acting directly on the pile and the load transferred by the soil around pile through the horizontal arch to the constraint pile, as shown in Fig. 10.

According to the equilibrium condition of the AEBB′E′A′ force in the plastic zone, it can be considered that the lateral horizontal force $p(z)$ of the soil layer acting on the pile horizontally is the difference in lateral horizontal force between the plane AA′ and the plane BB', and $P_{AA'}$ and $P_{BB'}$ are carried out according to formulas (1) and (2).

$$p_{AA'} = r_z N_\varphi^{-1} - 2cN_\varphi^{-1/2} \tag{1}$$

$$\begin{aligned} p_{BB'} = {} & D_1 \left(\frac{D_1}{D_2}\right)^{\left(N_\varphi^{\frac{1}{2}} \tan\varphi + N_\varphi - 1\right)} \\ & \left[\frac{1}{N_\varphi \tan\varphi}\left\{(\gamma z \tan\varphi + c)\right.\right. \\ & \times \exp\left(\frac{D_1 - D_2}{D_2} N_\varphi \tan\varphi \tan\left(\frac{\pi}{8} + \frac{\varphi}{4}\right)\right) \\ & \left.\left. - c\left(2N_\varphi^{\frac{1}{2}} \tan\varphi + 1\right)\right\}\right. \\ & + c\frac{2\tan\varphi + 2N_\varphi^{\frac{1}{2}} + N_\varphi^{-\frac{1}{2}}}{N_\varphi^{\frac{1}{2}} \tan\varphi + N_\varphi - 1}\Bigg] \\ & - c \cdot D_1 \frac{2\tan\varphi + 2N_\varphi^{\frac{1}{2}} + N_\varphi^{-\frac{1}{2}}}{N_\varphi^{\frac{1}{2}} \tan\varphi + N_\varphi - 1} \end{aligned} \tag{2}$$

The experimental results show that the settlement of the pile and soil in composite foundation can be effectively reduced with a lateral constraint. This is mainly because setting long piles with constraint stops the lateral deformations of soft soil in cement–soil pile composite foundations, thus reducing the settlement and improving the bearing capacity.

In Test 2, the ratio of the settlement value of the pile top to soil settlement is 42–53% with a constraint, which is 56–79% less than that in Test 1, and the settlement reduction in the soil in the composite foundation is 9%, which is larger than that in Test 1. The preliminary explanation is as follows: compared with Test 1, Test 2 is characterised by a large compressive modulus, high strength of soil and large pile spacing. In Test 2, the soil strength is high, and under the equal external load, the external load adjustment by cushion leads to the apportioning of more load to soil; correspondingly, the pile shares less load, so both the settlement of the pile and the ratio decrease. The lateral deformations of the composite foundation, which is subjected to the constraint pile, can reduce the settlement of the pile and soil. The cement–soil pile spacing is $3d$, which is larger than that in Test 1, and under the vertical load, the interaction between the pile is relatively small. However, in Test 2, high soil strength is beneficial to the formation of a horizontal soil arch, so the ratio of settlement value of the pile top to soil settlement with a constraint in Test 2 is even smaller than that in Test 1.

4.2 Pile Top Stress

When the soil strength is weak, the increased rate of pile top stress without constraint is higher than that with constraint. When the soil strength increases, the increase rate of the pile top stress with constraint is approximately the same as that without any constraint. This is mainly due to the increase in soil strength. Under the initial load, the settlement of soil is weak, and therefore, the cushion makes a very small adjustment, which exerts little stress on the pile and soil. On the other hand, without lateral constraint, the increase in external load causes the lateral deformations of soil from the composite foundation to increase, the settlement difference between the pile and soil increases, and hence, the pile must share more load compared to the foundation with constraint. Thus, in Test 1, the pile top stress of the piles without

constraint is obviously larger than that with constraint under equal loads.

4.3 Pile–Soil Stress Ratio

The main reason for the decrease in pile–soil stress ratio is that at the very beginning, the slight deformations of pile soil and cushion make a large diffusion area from the pile top to the load plate. Therefore, the pile is highly stressed, and the bearing capacity of the soil is small. The load increase causes an increase in cushion stress and settlement of the pile and soil; thus, the settlement difference of pile soil is larger, and the load transferred to the soil increases. Although the pile top load increases, its load proportion decreases. The law of the pile–soil stress ratio may be related to the pile spacing. When the pile spacing increases, the pile–soil interaction is slightly affected by the friction of the pile skin, and the soil occupies a larger proportion in the load sharing. Therefore, with an increase in the load, the pile–soil stress ratio is slightly lower than load of a small spacing composite foundation and quite similar.

4.4 Pile Shaft Stress

The maximum pile shaft stress appears at a certain depth below the pile top, which is mainly due to the settlement of the soil being greater than that of the pile, which causes negative friction of the pile. The larger the pile shaft stress is, the larger the settlement difference is. In general, the maximum pile shaft stress appears at an equal settlement plane, as shown in Fig. 8. It can be easily understood that the increase in settlement of the soil intensifies the downward force of equal settlement planes; that is, the position of maximum stress of the pile without constraint is below that with constraint under the same load. It is not clearly shown in Fig. 8 because there are not enough monitoring points.

Im [16] found that the maximum lateral stress of the soil appeared at 0.33 times the pile length by centrifugal testing. Chai [17] adopted PVD to improve Saga embankment soft soil and performed the measurements, which showed that maximum lateral deformation is 0.3 times the pile length. Thus, it is assumed that the maximum lateral displacement in Test 2 lies at 0.4 m. In the assumption that the pile with a constraint is a rigid body and that the pile with constraint can bear 70.6% of the horizontal lateral force at a depth of 0.4 m as calculated by formula (1) and (2), which can be approximately an elastic body before the soil enters the plastic stage; thus, the reduction in soil stress can show a corresponding reduction in displacement. The horizontal lateral force can be reduced half by considering the fixation of the bottom of the pile in the test consideration, that is, 50% of the maximum lateral displacement. Then, in Test 2, the settlement of the composite foundation can be reduced by 0.18 times. As in Reference [9,10], the maximum lateral displacement is 0.2–0.28 times the settlement in the centre, and the experimental result is basically consistent with that in the reference. The fixation of the bottom of the pile will better constrain the lateral deformations of the soil.

5 Conclusions

In the cement–soil pile composite foundation of the soft soil area, by setting lateral constraint on the pile foundation, the pile spacing of the constraint pile is two times the pile diameter. The results of the indoor model show the following under equal loads:

(1) Setting a lateral constraint upon a cement–soil pile composite foundation will reduce the settlement of the foundation, particularly the settlement reduction of the pile, because the lateral constraint stops the lateral deformations of soft soil. Comparing the settlement value without constraint and that of the cement–soil pile composite foundation, the settlement of the pile top is 8–30% lower, and the soil around the pile is 7–9% lower. With an increase in the soil strength and compression modulus, the settlement of soil with lateral constraint decreases dramatically.
(2) The pile top stress with constraint in the cement–soil composite foundation is 18–32% lower than that without constraint. The pile shaft stress of the cement pile first increases and then decreases with the depth, and the maximum stress appears at 0.15–0.35 times the pile length from the top. The position of the maximum stress of the pile without constraint is lower than that with constraint, and the maximum stress is 112–153% of the pile top stress. With an increase in the soil strength and modulus, the pile top stress with constraint and without constraint tends to be the same.
(3) The pile–soil stress ratio decreases with the increase in the load, and under equal load and cushion thickness, the pile–soil stress with lateral constraint is 14–40% lower than without lateral constraint. With the increase in the soil strength and modulus, the pile–soil stress ratio with lateral constraint decreases slightly compared with that without constraint.

Therefore, setting a lateral constraint on a soft pile composite foundation can effectively reduce the settlement and improve the bearing capacity of the soil, thereby improving the bearing capacity of the composite foundation.

Acknowledgements Financial supports from the National Natural Science Foundation of China (No. 51108176) are sincerely acknowledged.

References

1. Liu, F.; Fan, B.J.; Zhang, T.: Analysis on subgrade treatment of Shenyang–Dandong passenger dedicated line with flexible piles. Bridge Tunn. Constr. Mach. **30**(11), 104–106 (2013)
2. Zeng, C.X.; Cheng, Y.; Wu, D.L.: Comparison of different foundation treatment effects on thick sand overlying thick silt foundation of high speed railway. China Railw. Sci. **35**(4), 1–8 (2014)
3. http://news.gaotie.cn/jianshe/2016-05-19/325352.html [EB/OL]. Accessed 19 May 2016
4. Tavenas, F.; Leroueil, S.: Effects of stresses and time on yielding of clays. Jpn. Soc. Soil Mech. Found. Eng. **1**, 319–326 (1977)
5. Handy, R.L.: Does lateral stress really influence settlement. Geotech. Geoenviron. Eng. **127**(7), 623–626 (2001)
6. Wang, Z.L.; Li, Y.C.; Yin, Z.Z.: Discussion on settlement calculation of embankment considering lateral dilation behavior of soil. Chin. J. Rock Mech. Eng. **24**(10), 1772–1777 (2005)
7. Wang, F.; Jin, W.; Wang, H.K.: Amendment of subgrade settlement of passenger dedicated line considering the lateral deformation effects. Chin. J. Geotech. Eng. **32**(Sup. 2), 245–248 (2010)
8. Smadi, M.M.: Lateral Deformation and Associated Settlement Resulting from Embankment Loading of Soft Clay and Silt Deposits. University of Illinois at Urbana–Champaign, Urbana (2001)
9. Loganathan, N.; Balasubramaniam, A.S.; Bergado, D.T.: Deformation analysis of embankments. J. Geotech. Eng. **119**(8), 1185–1206 (1993)
10. Han, J.L.; Zhao, Y.: Analysis on the settlement characteristic of lateral displacement of the high embankment. J. Wuhan Univ. Technol. (Transp. Sci. Eng.) **36**(1), 165–167 (2012)
11. Liu, J.; He, J.; Tan, J.: Influencing factors of lateral extrusion on soft soil in composite foundation with flexible columns. J. Cent. South Univ. (Sci. Technol.) **45**(7), 2333–2338 (2014)
12. Wu, B.Q.: Study on the Principles and Technical Methods for Grid Composite Foundation in Silt. Chengdu University of Technology, Chengdu (2008)
13. Bai, S.P.; Chen, X.P.; Li, Y.L.: Study of soft soil treatment technology of lateral restraint. Highway **7**, 127–130 (2005)
14. Wu, Y.P.; Liu, J.; He, J.: Experiment and study on the stress testing of cement–soil piles. J. Hunan Univ. Technol. **26**(1), 23–26 (2012)
15. Ito, T.; Matsui, T.: Methods to estimate lateral force acting on stabilizing piles. Soils Found. **15**(4), 43–59 (1975)
16. Im, E.S.; Tai, H.K.: Lateral earth pressure acting on underground retaining structure in clay ground under embankment based on centrifuge model tests. KSCE J. Civ. Eng. **8**(4), 387–396 (2004)
17. Chai, J.; Carter, J.P.: Modelling Soft Clay Behaviour. Deformation Analysis in Soft Ground Improvement, pp. 7–55. Springer, Dordrecht (2011)